Available online at www.sciencedirect.com

SCIENCE DIRECT

Biochimica et Biophysica Acta 1707 (2005) 24–33

BIOCHIMICA ET BIOPHYSICA ACTA
BBA

http://www.elsevier.com/locate/bba

Review

C–C bond formation and cleavage in radical enzymes, a theoretical perspective

Fahmi Himo*

Theoretical Chemistry, Department of Biotechnology, Royal Institute of Technology, ALBANOVA, SE-106 91 Stockholm, Sweden

Received 28 April 2003; accepted 19 April 2004
Available online 8 May 2004

Abstract

Quantum chemical methods are today a viable tool in the study of enzyme catalysis. The development of new density functional techniques and the enormous advancement in computer power have made it possible to accurately describe active sites of enzymes. This review gives a brief account of the methods and models used in this field. Three specific enzymes are discussed: pyruvate-formate lyase (PFL), spore photoproduct lyase (SPL), and benzylsuccinate synthase (BSS). What these enzymes have in common is that they use radical chemistry to catalyze C–C bond formation or cleavage reactions.

Keywords: Density functional theory; Pyruvate-formate lyase; Spore photoproduct lyase; Benzylsuccinate synthase; Radical enzyme

1. Introduction

In recent years, significant progress has been made in understanding, at the molecular level, the structure and function of radical enzymes. X-ray crystal structures have been solved for a number of them and the active sites have been characterized by an array of different spectroscopic methods.

Parallel with these advancements, quantum chemical methods have quite recently reached the level of speed and accuracy that makes them a valuable tool in the study of enzyme mechanisms. This relies on several factors. Probably the most important one is the development of the density functional theory (DFT) approach. In the last decade, DFT has improved from being a method providing qualitative results to becoming a quantitatively highly accurate method, competing with the most accurate ab initio methods. To a large extent, this depends on the development of gradient-corrected functionals, and recently also so-called hybrid functionals that include a fraction of Hartree–Fock exchange and a few semi-empirical parameters [1–4]. The most commonly used functional, the so-called B3LYP, for instance, has an average deviation to experiments of 0.013 Å on bond distances and 2.2 kcal/mol on atomization energies, when benchmarked against a standard set of molecules [5].

The favorable scaling (i.e. the computational effort with the system size) of DFT compared to ab initio methods allows for the treatment of far larger systems, and has thus opened the door to much wider applications than ever before. Of course, the nearly exponential development in computer power also has a major impact on the field. Quantum chemistry has gone from being a quite expensive branch of science to quite a cheap one, where many problems can be addressed using a few ordinary personal computers.

One of the major advantages of theoretical studies compared to experiments is that short-lived intermediates can be located and studied with the same straightforward methods as stable ones. In the field of radical enzymes, this is of course particularly valuable. On the other hand, a major disadvantage is the size of the systems that can be treated. With the computer power of today, one is able to treat systems of up to 100 atoms with accurate methods. Although it is a huge improvement compared to just a couple of years ago, this size poses some limitations and implies constant trade-off considerations.

Very recently, the field of quantum chemical applications to radical enzymes was comprehensively reviewed [6]. In

* Tel.: +46-8-553-78-415; fax: +46-8-553-78-590.
E-mail address: himo@theochem.kth.se (F. Himo).

0005-2728/$ - see front matter © 2004 Elsevier B.V. All rights reserved.
doi:10.1016/j.bbabio.2004.04.006

the present review, we focus our attention on a sub-class of these enzymes, namely those catalyzing C–C bond formation or cleavage. Three enzymes are considered: pyruvate-formate lyase (PFL), spore photoproduct lyase (SPL), and benzylsuccinate synthase (BSS). Only the most necessary experimental information will be given for these systems. The methodology used will be briefly discussed first. For a more extended discussion on the accuracy of the methods and the limitation of the models used in the study of enzymatic catalysis, see recent reviews [7–10].

2. Methodology

2.1. Chemical models

In any quantum chemical study, it is essential to choose the models to accurately represent the chemical situation. To test one or several reaction pathways and to find the transition states connecting the intermediates, a large number of calculations are usually required. With an active site of an enzyme containing four to five amino acids, we are immediately up to sizes on the limit of what can be handled within reasonable time with the computer power of today. Hence, the need arises to employ as small models as possible of the active sites, in order to limit the computational time. At the same time, we have to ensure that the basic chemical features of the system are correctly accounted for. Let us illustrate this issue with a couple of very simple examples.

Amino acid radicals are created by hydrogen atom abstraction from their side chain. Thus, one very important property that needs to be modeled correctly in the study of radical enzymes is the energy required to create the radicals, i.e. the X–H bond dissociation energy (BDE) of the amino acid side chains. The examples given here are concerned with the amino acids of cysteine and tyrosine.

The full cysteine residue, $NH_2(COOH)CHCH_2SH$, has a calculated (B3LYP/6-311+G(2d,2p)) S–H BDE of 81.7 kcal/mol (see Table 1). The smallest model of cysteine is H_2S, for which the S–H BDE is calculated to 87.1 kcal/mol, an overestimation by 5.4 kcal/mol. A larger, but still quite small, model is methylthiol, CH_3SH. The calculated S–H BDE for this species is 81.9 kcal/mol, only 0.2 kcal/mol from the BDE of the full residue. Adding another methyl group will not give any significant change of the BDE (Table 1). The calculated S–H bond strength of ethylthiol, CH_3CH_2SH, is in fact identical to that of methylthiol. Thus, to model the S–H BDE of cysteine, it is sufficient to use CH_3SH. This result reflects the fact that the spin in the cysteine radical is localized to the sulfur center, lacking any kind of resonance delocalization. The Mulliken spin densities on the sulfur atom for $HS^{\cdot}$, $CH_3S^{\cdot}$, $CH_3CH_2S^{\cdot}$ and the full cysteine radicals are 1.03, 0.98, 0.98 and 0.98, respectively.

Table 1
Calculated (B3LYP) S–H and O–H bond strengths (kcal/mol) for different models of cysteine and tyrosine

Model	Bond strength
S–H	
H_2S	87.1
CH_3SH	81.9
CH_3CH_2SH	81.9
Full cysteine	81.7
O–H	
H_2O	114.4
CH_3OH	99.4
Vinyl alcohol	81.6
Phenol	83.1
Full tyrosine	82.2

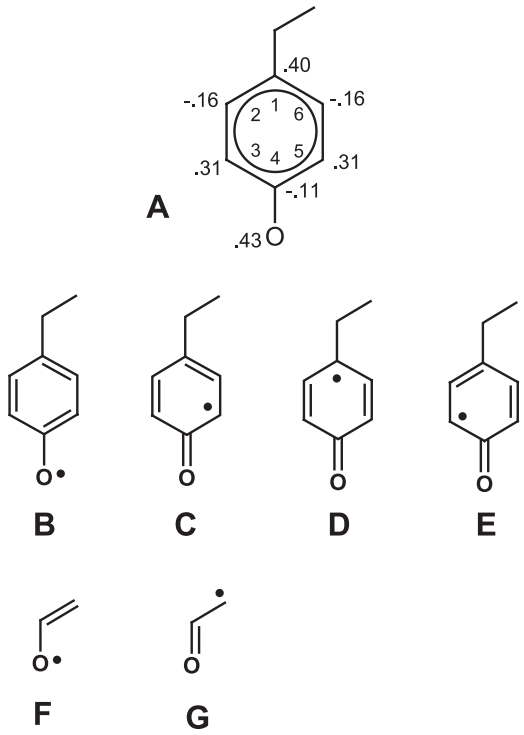

Scheme 1. Calculated spin distribution of tyrosyl (A) and principal resonance structures of tyrosyl (B–E) and vinyl alcohol radicals (F–G).

A system where spin delocalization and resonance stabilization is predominant is the tyrosyl radical (Scheme 1). The spin in this π-radical is delocalized over the aromatic ring and exhibits a well-characterized odd-alternant spin pattern, with the oxygen and the 1-, 3-, and 5-carbons having large positive spins, and the 2-, 4-, and 6-carbons small negative spins. Clearly, water (H_2O) or methanol (CH_3OH) cannot account for any of these resonances, the calculated O–H bond strengths are much larger in these molecules (114.4 and 99.4 kcal/mol for water and methanol,

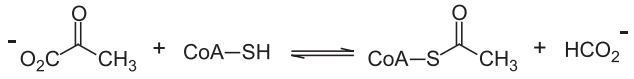

Scheme 2. Reaction catalyzed by PFL.

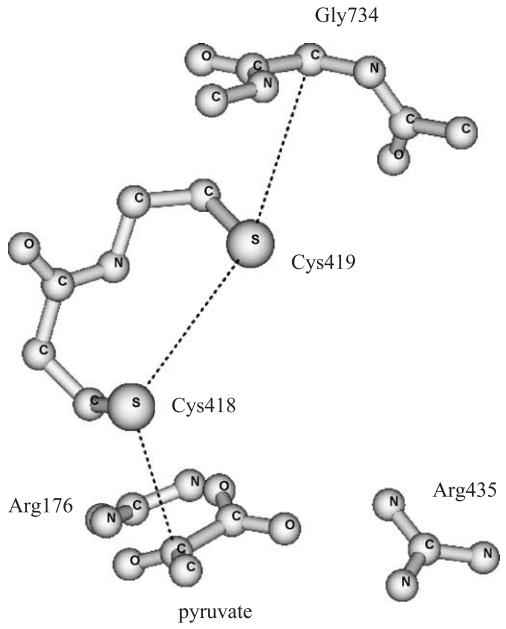

Fig. 1. X-ray structure of the active site of PFL in complex with the substrate [15].

respectively), compared to the full tyrosine residue (82.2 kcal/mol), see Table 1. Instead, a natural choice of model is phenol, which has a calculated BDE of 83.1 kcal/mol. The neglect of the rest of the amino acid leads hence to an increase of the BDE by modest 0.9 kcal/mol, which is a comparatively cheap accuracy price to pay. An even smaller model that works surprisingly well is vinyl alcohol. The resonance structures in this radical (Scheme 1) resemble those in the full tyrosine to such an extent that the calculated BDEs only differ by 0.6 kcal/mol (Table 1).

Similar analysis can be done to develop models of the other amino acids. For instance, for many purposes, imidazole has been found to be an adequate model of histidine, formic acid for aspartic and glutamic acids, methanol for serine, and indole for tryptophan.

To model metal centers, normally only the first coordination shell needs to be included. This usually defines the essential characteristics of the metal site. If some second shell residues are experimentally known, or can be suspected, to influence the reactions, they are included explicitly. In cases where the metal site is particularly large, including several metal centers, some of the ligands that do not directly participate in the chemistry can be replaced by simpler ligands, such as water or ammonia, as a first approximation.

This systematic build-up of models is not only important for speeding up the calculations, it also enables identification and understanding of important factors contributing to the characteristics of the system. This, in a sense, is one of the major points in doing calculations. Hence, bigger is not always better. Starting directly with a large model can also cause problems with local minima, which could have severe consequences on the energetics.

2.2. Solvation effects

There are different types of effects induced by the solvent (or in this case the protein surrounding). Solvent molecules can be part of the reaction, like for instance in hydrolysis reactions. In this case, the only way to model the situation

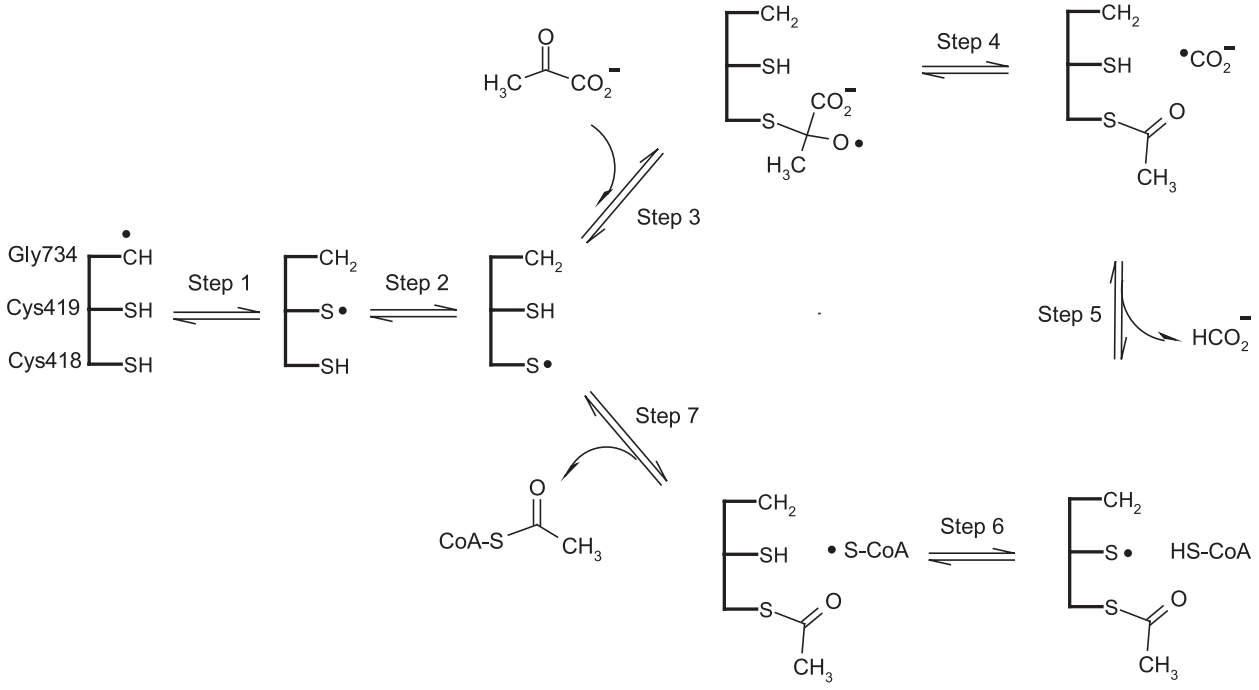

Scheme 3. Currently accepted reaction mechanism for PFL.

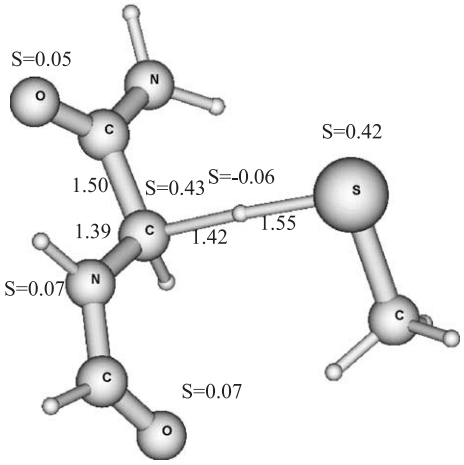

Fig. 2. Optimized transition state structure for the direct hydrogen atom transfer from cysteine to glycyl radical.

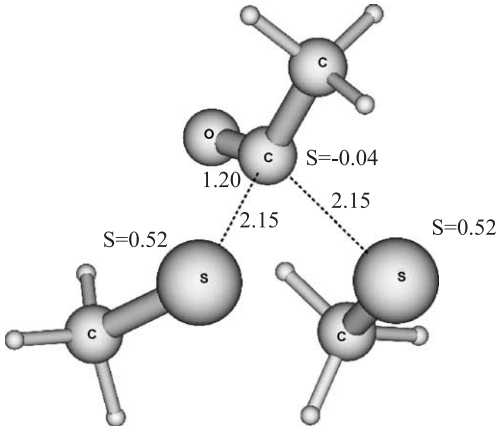

Fig. 4. Optimized structure and spin population distribution of the transition state of the homolytic acetyl transfer between cysteine and CoA.

is, of course, to include the parts that are needed in the quantum calculation. The same applies to short-range solvent effects, where, for instance, strong hydrogen bonds are known to form or break during the course of the reaction.

The rest of the enzyme is usually considered as a homogeneous polarizable medium and can normally be modeled by dielectric cavity techniques. In these methods, the solute cavity is determined from a surface of constant charge density around the solute molecule. The dielectric constant chosen for proteins is the standard $\varepsilon = 4$. The relative solvent effects between minima and transition states are normally calculated to be quite small (on the order of a few kilocalories/mol), which makes the particular choice of the dielectric constant less critical. Typically, when large solvent effects are obtained, it is indicative of some deficiency in the chemical models that need to be corrected. The solvation energies are usually calculated as single points on top on the gas-phase optimized geometries.

Another effect of the enzyme surrounding can be steric. The enzyme environment can prevent a certain group from moving in a certain way or from making a certain rotation. Two strategies can be used to deal with this. A simple procedure that has recently become popular is to fix a number of atoms at the edge of the quantum chemical model, corresponding to where the rest of the enzyme is cut. Another procedure is to use so-called QM/MM methods, where the active site is described using quantum mechanical (QM) methods and the surrounding is treated with classical molecular mechanics (MM).

2.3. Transition state theory

A rather simple, and at the same time very powerful, way to connect the calculated barriers to experimental rates is by means of classical transition state theory. The central assumption here is that the transition structure is in rapid equilibrium with the reactants. This allows the derivation of the following basic formula

$$k = \frac{k_B T}{h} e^{-\Delta G/RT}$$

where ΔG is the difference in the Gibbs free energy between the transition state and the reactants, T is the absolute

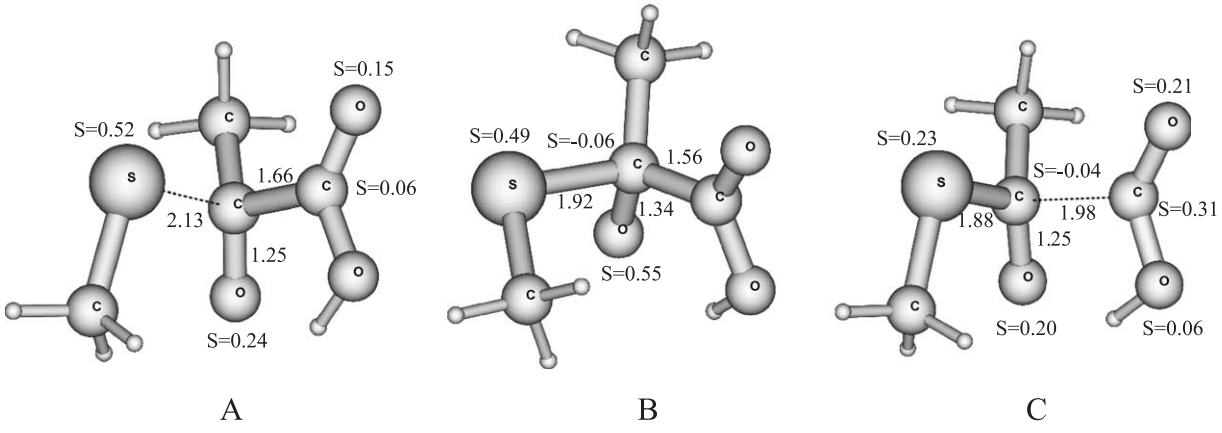

Fig. 3. Optimized structures for (A) the transition state for the thiyl radical addition to pyruvate, (B) the tetrahedral oxy-radical intermediate, and (C) the transition state for the dissociation of formyl radical. Important distances (Å) and spin densities are given.

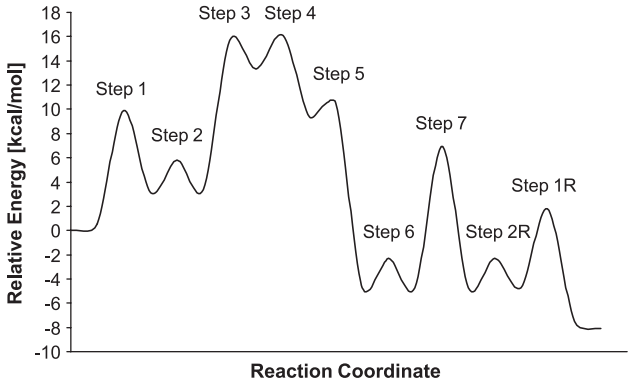

Fig. 5. Calculated potential energy surface for the reactions of PFL. Steps 1R and 2R are the reverse of Steps 1 and 2 in Scheme 3, respectively.

temperature, R is the gas constant, k_B is the Boltzmann constant, and h is Planck's constant. At room temperature, a barrier of ca. 18 kcal/mol corresponds to a rate constant of ca. one per second. Another useful rule of thumb is that for every increase (or decrease) of 1.4 kcal/mol in the barrier, the rate decreases (or increases) by one order of magnitude. From this, we can immediately see that the accuracy of the theoretical method used here does not allow for accurate determination of rate constants. An error of 3 kcal/mol in the calculated barrier, which is a quite small error in this context, corresponds to an error of two orders of magnitude in the rate.

Practically, locating a transition state (TS) structure is a bit tricky and relies to a certain degree on experience and chemical intuition. Every problem is unique, with its own peculiarities. There is however a general scheme that can be used and that is very helpful in many cases. It can be described in the following way: first, one degree of freedom is identified and chosen as a reaction coordinate. In the case of C–C bond formation and cleavage (the subject of this paper), the obvious choice is the C–C bond distance. In other situations, it could be more complicated to choose a proper reaction coordinate, especially in the case of concerted reactions, where more than one degree of freedom is involved. Once the reaction coordinate is chosen, a linear transit scheme can be applied. That is, the value of the reaction coordinate is kept fixed in steps while all other degrees of freedom are minimized. This way, the energy maximum along the reaction coordinate, and thus the TS region can be located, and a qualified starting structure for the transition state optimization is obtained. For the TS optimization procedure, a Hessian matrix is typically required. The Hessians are computationally rather expensive, and it is typically sufficient to calculate the Hessian for the TS optimization at a lower level, such as Hartree–Fock with a rather small basis set.

A general insight that has been gained from experience is that the local structure of the TS is quite insensitive to the size of the chemical model employed. The quite demanding and tedious search for the TS can thus be done using as small model as possible, and the local geometry can then be transferred to the extended model to obtain accurate energetics.

3. Pyruvate-formate lyase

PFL was the first enzyme discovered to harbor a stable glycyl radical [11,12]. It catalyzes the reversible conversion of pyruvate and coenzyme A (CoA) into acetylated CoA and formate (Scheme 2), a reaction that is a key component of the anaerobic carbon metabolism in *Escherichia coli* and other prokaryotes. In addition to the glycyl radical, two other residues are known to be essential for catalysis, namely Cys418 and Cys419.

The X-ray crystal structure of PFL was recently solved [13–15] (active site shown in Fig. 1). It shows that the Gly734 in close proximity to Cys419, and the position of the substrate implies that Cys418 is the residue performing the attack on pyruvate.

Based on the crystal structure and numerous biochemical, spectroscopic, and also theoretical studies, the following mechanism is the currently accepted one (Scheme 3). The first two steps involve hydrogen atom transfers, first from the Cys419 to the glycyl radical, and then from Cys418 at the substrate binding site to Cys419. This kind of hydrogen transfer is now believed to be a paradigm in glycyl radical enzymes, i.e. the glycine residue serves as a site for radical storage, and starts catalysis by abstracting a hydrogen atom from a neighboring cysteine, which then activates the substrate. Next, the Cys418 radical adds to the keto group

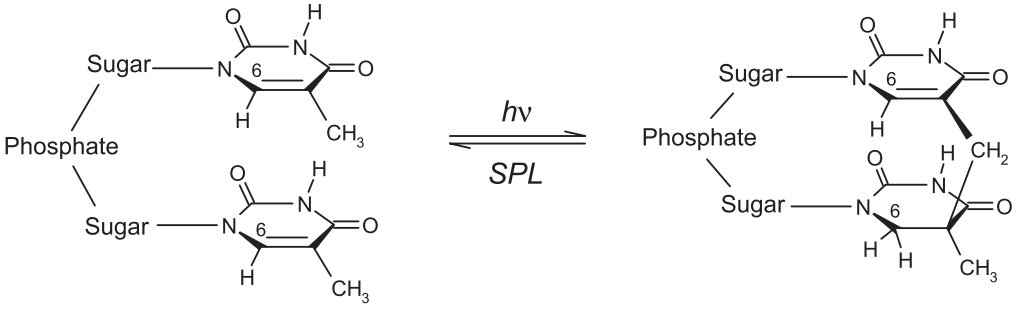

Scheme 4. Reaction catalyzed by SPL.

of pyruvate forming a tetrahedral oxy-radical intermediate, which subsequently collapses into an acetylated cysteine and a formyl radical. The formyl radical then abstracts a hydrogen atom from Cys419, which in turn abstracts the thiol hydrogen atom from CoA-SH. This way, the acetyl group transfer between Cys418 and CoA in the next step becomes facile. At this point, the reaction is completed, and the enzyme can either take a new substrate or regenerate the stable glycyl radical by a hydrogen atom transfer chain.

In the DFT calculations [16] (which were performed prior to the crystal structure), the glycine was modeled using a CHO-NH-CH_2-CO-NH_2 molecule. It was found necessary to include the peptide bonds from the neighboring residues in order to reproduce the C–H bond strength correctly [17,18]. For cysteine, CH_3SH was used in accordance with the discussion above. Furthermore, the carboxylate moiety of the pyruvate substrate was protonated. The reason for this is that these negatively charged carboxylate groups are typically found to hydrogen bond to positively charged groups in the proteins, in this case to an arginine side chain.

The C_α–H bond strength of protein-bound glycine is well-tuned for its activity. The glycyl radical is 3.4 kcal/mol more stable than the cysteinyl radical, making the latter readily accessible when needed upon substrate binding. The barrier for the direct hydrogen transfer reaction between cysteine and glycyl (Step 1) was calculated to the very feasible 9.9 kcal/mol (optimized transition state structure is displayed in Fig. 2). Step 2 is thermoneutral and has a very small barrier of 2.4 kcal/mol.

Steps 3 and 4 are the crucial ones, where the S–C bond is formed and the C–C bond is broken. This, at the time controversial, mechanism was originally proposed by Kozarich et al. [19,20], and substantiation came later by DFT calculations [16]. The addition of the thiyl radical to the carbonyl carbon of pyruvate to give the tetrahedral oxy-radical intermediate was indeed shown to be energetically very plausible. The barrier was calculated to 12.3 kcal/mol, and the intermediate was found to be in a shallow well, only 2.4 kcal/mol lower than the transition state. The barrier for its dissociation into acetylated cysteine and formyl radical was calculated to be only 2.8 kcal/mol with an exothermicity of 3.9 kcal/mol, giving an overall endothermicity of 6.0 kcal/mol, Steps 3 and 4 together. The optimized structures of the tetrahedral radical intermediate and the transition states for its creation and collapse are shown in Fig. 3.

The dissociation of the formyl radical can be rationalized in terms of hyperconjugation, which is the stabilizing effect caused by the interaction of the singly occupied p-orbital with the σ-orbital of the C–C bond to be broken. As seen from Fig. 3B, the spin in the tetrahedral radical intermediate is shared between the oxygen and the sulfur centers, both of which adopt a nearly perpendicular arrangement relative to the C–C bond, maximizing the overlap between these orbitals. The hyperconjugation gets stronger and stronger as the C–C bond is broken, thereby lowering the barrier for that cleavage. Furthermore, the simple fact that the formyl radical is much more stable than the methyl radical explains

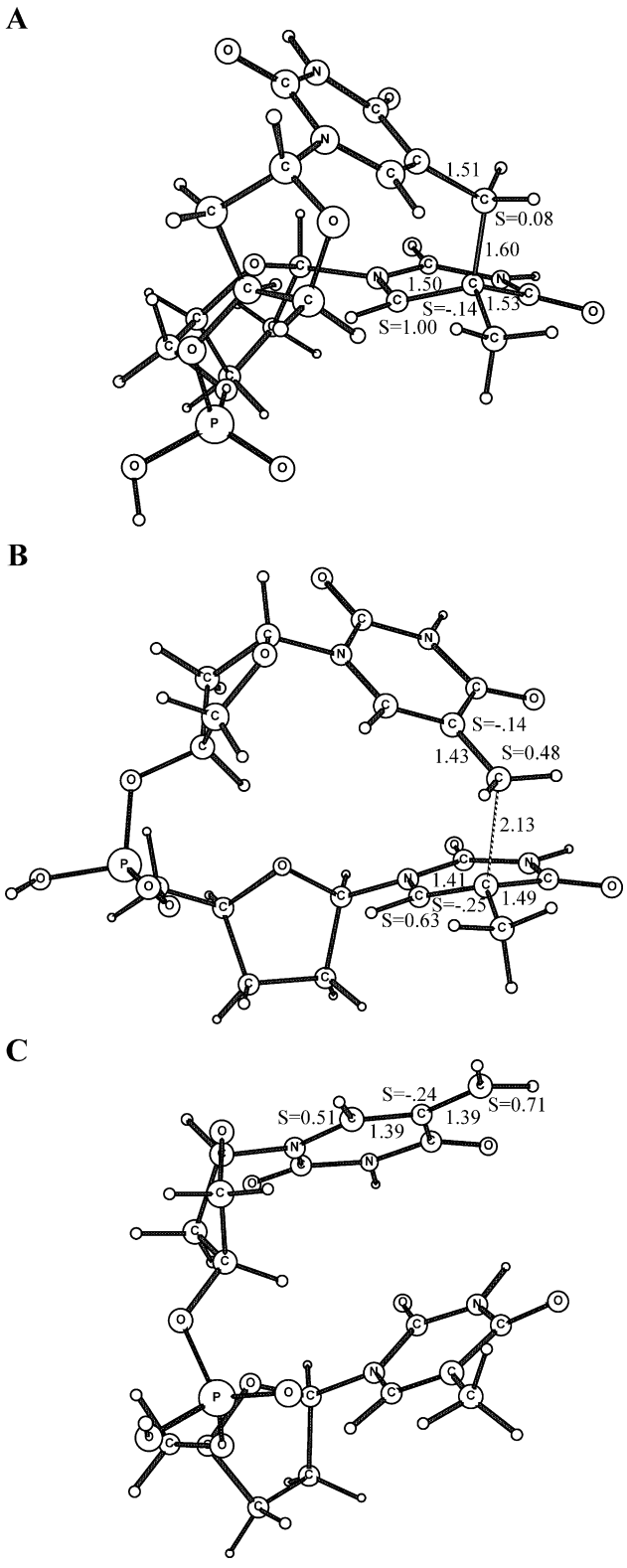

Fig. 6. Optimized structures of the dimer radical before (A), at the transition state (B), and after (C) the C–C bond cleavage.

why the C–C bond to the methyl group of pyruvate does not dissociate, although experiencing the same hyperconjugative effect.

The formyl radical was, based on the DFT calculations, proposed to be quenched by a cysteine residue, with a calculated barrier of 1.1 kcal/mol and an exothermicity of 14.1 kcal/mol. In the next step, the Cys419 radical is proposed to abstract a hydrogen from CoA-SH (barrier 2.4 kcal/mol). Having created the CoA radical, the proposed acetyl group transfer between Cys418 and CoA is now energetically plausible, with a barrier of the quite reasonable 11.6 kcal/mol (transition state structure in Fig. 4).

The final steps are to regenerate the glycyl radical by hydrogen atom transfers, first between Cys418 and Cys419, and then between glycine and Cys419. These steps are the reverse of the first and second steps, respectively. The potential energy surface for the full reaction is presented in Fig. 5.

The mechanism of PFL is currently being revisited using much larger models based on the X-ray structure [21].

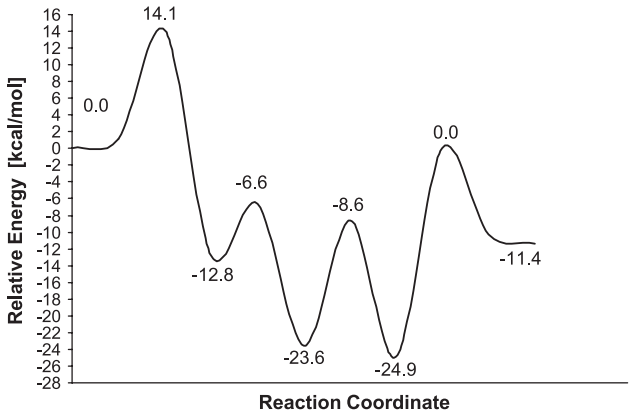

Fig. 7. Calculated potential energy surface for the reactions of SPL.

4. Spore photoproduct lyase

SPL is an iron–sulfur enzyme that uses *S*-adenosylmethionine (AdoMet) as a cofactor to catalyze the repair of thymine dimers created in the DNA of UV-irradiated bacterial spores (Scheme 4).

Based on model experiments, Mehl and Begley [22] proposed the following mechanism for SPL. The 5′ dAdo radical initiates the repair by abstracting the C6 hydrogen atom of the spore photoproduct. The C–C bond linking the two pyrimidines is weakened by this hydrogen atom abstraction and undergoes then β-scission. The last step is the transfer of the hydrogen atom back from the 5′ dAdo to the thymine monomer radical, completing the repair. Recent

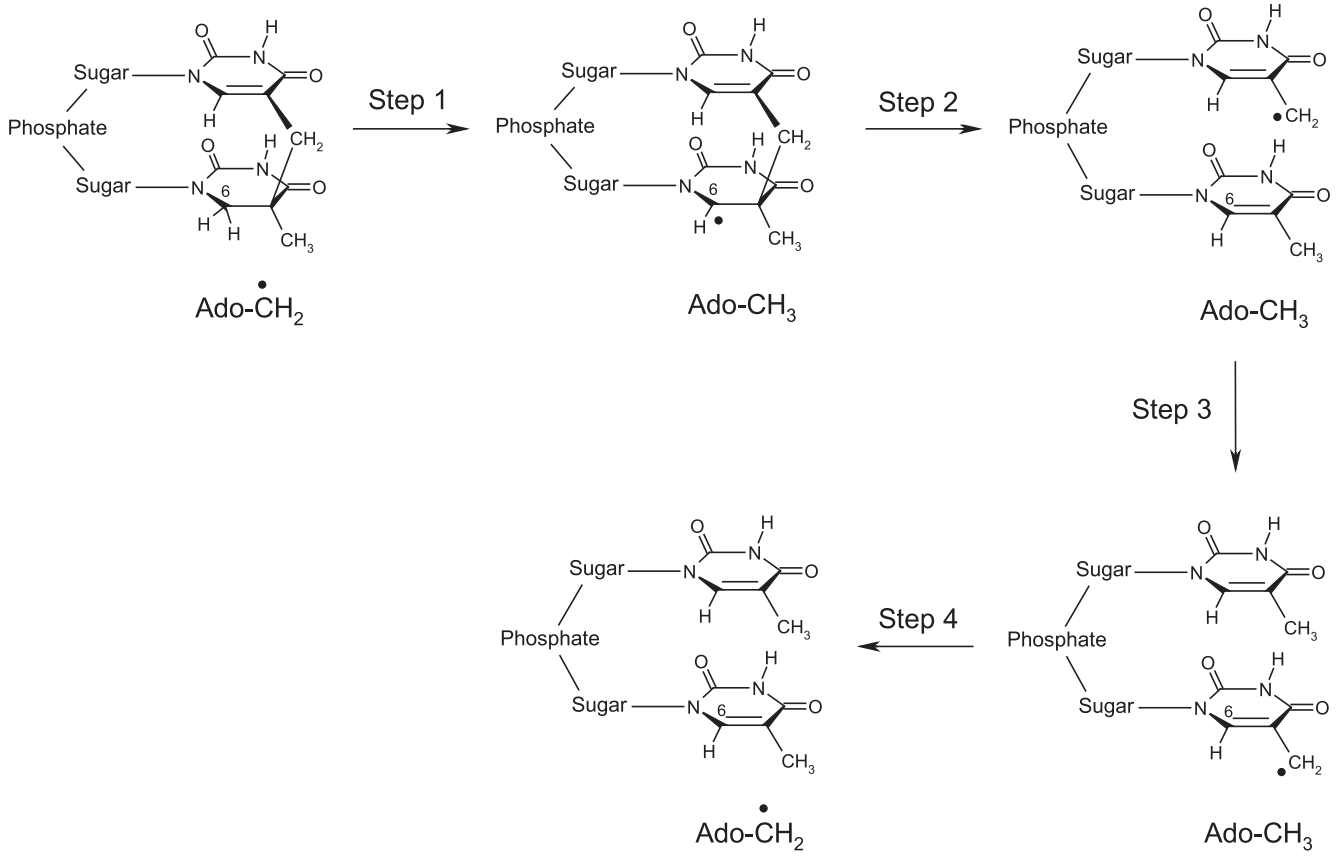

Scheme 5. Proposed reaction mechanism of SPL.

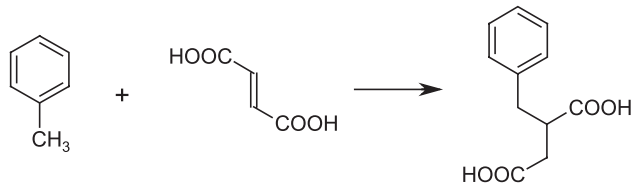

Scheme 6. Reaction catalyzed by BSS.

isotope labeling experiments [23] gave support to this mechanism. In these experiments, spore photoproduct, specifically ^{3}H-labeled at the C6 position, was shown to transfer label to adenosylmethionine during repair. Further support to the existence of the 5′ dAdo radical was given by electrospray ionization mass spectroscopy and HPLC experiments [24].

This mechanism was recently tested by means of DFT calculations [25]. The thymine dimer was modeled using the two bases and the DNA backbone linking them (two sugars and a phosphate group), as shown in Fig. 6. As there is no structural information about the system, the molecule had to be built from scratch starting from standard B-form DNA structure. The 5′ dAdo radical was modeled using a ribose ring, where a hydrogen atom replaced the 2-adenine.

The first step (hydrogen atom transfer from C6 of the thymine dimer to the 5′ dAdo radical) was calculated to have a quite feasible barrier of 14.1 kcal/mol. The step is exothermic by 12.8 kcal/mol, which is the BDE difference between C–H of 5′ dAdo and the C6–H of the dimer.

In the resulting dimer radical intermediate (Fig. 6A), the C–C bond length is 1.60 Å, slightly longer than C–C single bond in the non-radical species (1.58 Å). This is indicative of a hyperconjugation destabilization of the bond. The barrier to break this bond is calculated to be very low, only 6.2 kcal/mol, and the step is exothermic by 10.8 kcal/mol. At the transition state (Fig. 6B), the C–C bond is 2.13 Å and the spin is distributed over the two thymine rings. After the bond cleavage, the spin is concentrated to one of the rings (see Fig. 6C).

As in the case of PFL, hyperconjugation can be used to explain the weakening of the C–C bond. Again, the thymine monomer radical is much more stable than the methyl radical, explaining why this C–C bond is broken and not the one to the methyl group.

The final step in the proposed mechanism is the back transfer of the hydrogen atom from 5′ dAdo to the thymine monomer radical, quenching the DNA radical and regenerating the 5′ dAdo radical.

Comparing the position of the 5′ dAdo cofactor relative to the DNA when abstracting the hydrogen and delivering it back, it is difficult to envision how the cofactor can move from one end of the system to the other to affect both hydrogen transfer steps.

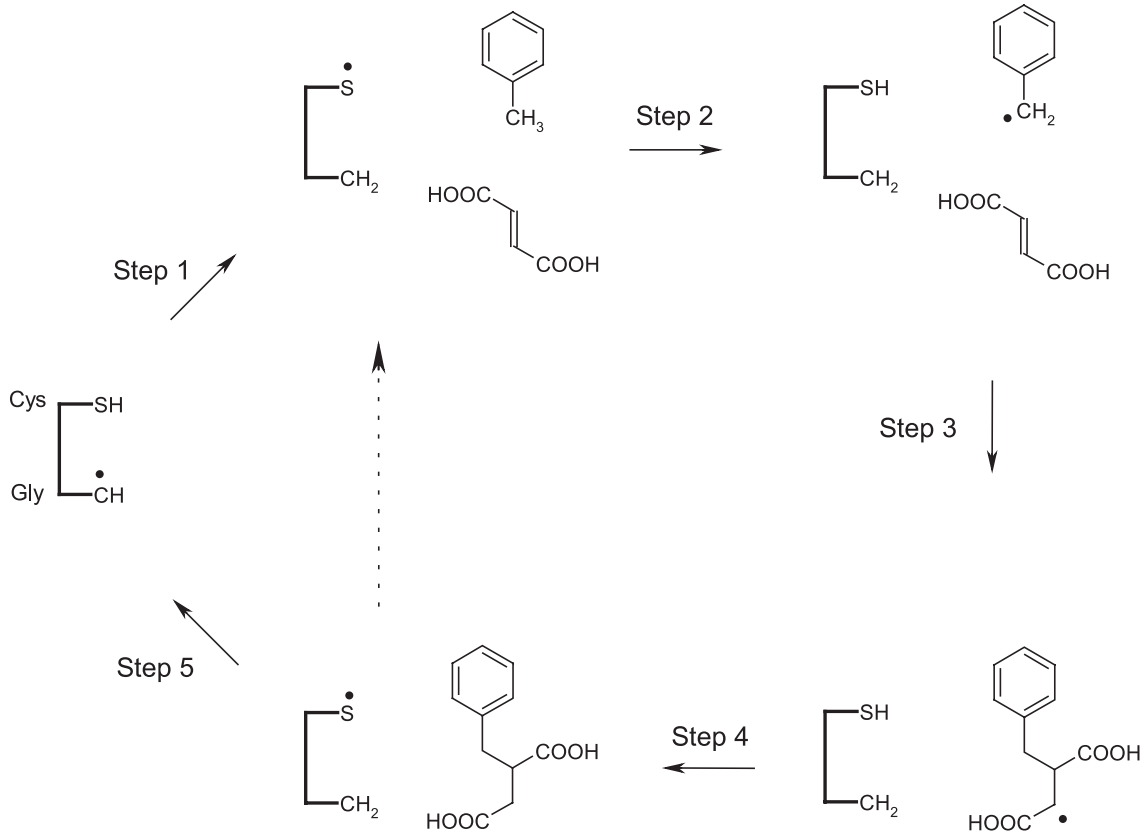

Scheme 7. Proposed reaction mechanism for BSS.

The calculations instead suggest a slightly different path. A hydrogen atom transfer is proposed to take place from the methyl group of one thymine to the methyl radical of the other, before a hydrogen can be abstracted from 5′ dAdo, as displayed in Scheme 5. The barrier for the almost thermoneutral inter-thymine hydrogen transfer is calculated to be 15.0 kcal/mol.

In the last step, the hydrogen atom from 5′ dAdo to the thymine monomer radical is quite endothermic (by 13.5 kcal/mol) due to the difference in BDE between the two. This results in a reaction barrier of rather high 24.9 kcal/mol, which makes this step the rate-limiting one of the reactions considered here (see Fig. 7). A barrier of 25 kcal/mol is higher than what can be accepted for enzymatic reactions. This is believed to be an overestimation because the ground state is overstabilized due to the relatively small model employed using only two bases of the DNA sequence. Another possibility is that this step is coupled to some energetically favorable step following, like for instance the recombination of the Ado radical with the methionine, to regenerate the AdoMet cofactor.

5. Benzylsuccinate synthase

BSS catalyzes the addition of toluene to fumarate, forming benzylsuccinate (Scheme 6). This reaction initiates the anaerobic toluene degradation in denitrifying bacteria.

BSS was first suggested to contain a glycyl radical on the basis of strong homology between the α-subunit and PFL and anaerobic ribonucleotide reductase (ARNR) [26]. The existence of the glycyl radical in BSS was recently established by means of EPR spectroscopy [27]. The mechanism displayed in Scheme 7 has been proposed for BSS [26,27]. First, the stable glycyl radical abstracts a hydrogen atom from a neighboring cysteine residue, creating a transient thiyl radical. This step is identical to the first step in the PFL reactions. The thiyl radical then abstracts a hydrogen atom from the toluene methyl creating a benzyl radical intermediate. This benzyl radical then attacks the double bond of the fumarate, yielding a benzylsuccinyl radical intermediate, which is subsequently quenched by hydrogen atom transfer from the cysteine, giving the benzylsuccinate product. The cysteinyl radical then either abstracts a hydrogen atom from the glycine residue, regenerating the stable glycyl radical, or starts a new catalytic cycle by abstracting a hydrogen atom from a new toluene substrate.

The thermodynamic and kinetic feasibility of this mechanism was tested recently by DFT calculations [28]. Since the crystal structure of BSS has not yet been solved, the calculations included only the substrates and the active glycine and cysteine residues. It was indeed shown that the proposed mechanism is plausible in that all steps were shown to have favorable reaction energies and activation barriers.

The rate-limiting step was found to be the addition of benzyl radical to fumarate (Step 3 of Scheme 7), with a total barrier of 15.0 kcal/mol. Optimized structures of the C–C formation transition state and the resulting benzylsuccinate radical intermediate are shown in Fig. 8.

The two hydrogen atom transfer steps preceding the C–C bond formation have relatively low barriers (10.7 and 12.9 kcal/mol, respectively). The benzyl radical is stabilized by resonances similar to those in phenoxyl, lowering the toluene C–H bond dissociation energy and hydrogen transfer barrier. The benzylsuccinyl radical is quenched by the cysteine (barrier 7.0 kcal/mol) and the glycyl radical is

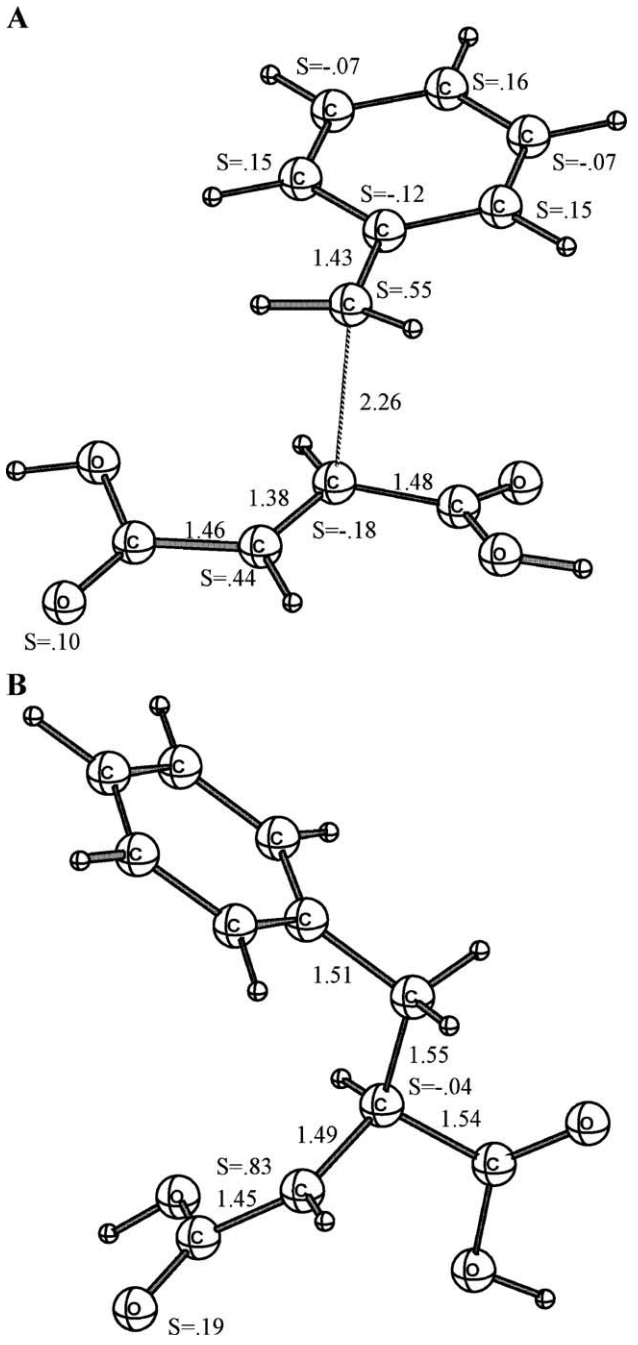

Fig. 8. Optimized structures for the C–C formation transition state (A) and the resulting benzylsuccinyl radical (B).

finally regenerated in a step that is the reverse of the first step.

6. Conclusions

Comprehensive understanding of enzymatic catalysis requires detailed knowledge about the geometric and electronic structures of the active site of the enzyme. Theoretical methods have in the last few years started to have impact on this field, a development that undoubtedly will continue with even greater momentum over the coming years. With modern density functional methods, it is now possible to accurately study systems large enough to model active sites of proteins in a quite reasonable way. Mechanisms can be substantiated or refuted on the basis of their thermodynamic feasibility. Theory can also help proposing new mechanistic pathways. The present review has tried to give some examples of this. We have focused on three radical enzymes that catalyze C–C bond formation or cleavage; pyruvate-formate lyase, spore photoproduct lyase, and benzylsuccinate synthase.

For example, for the reactions of BSS, the calculations gave a clear confirmation of the experimentally proposed mechanism. The energies and barriers of all steps were found to be plausible. In PFL, it was shown that the Kozarich mechanism involving the tetrahedral radical intermediate is energetically favorable, and a new pathway in which the acetyl transfer to CoA proceeds through a radical step was proposed based on the calculations. For SPL, the C–C bond breaking step was found to have a very low barrier, once the radical is created at the thymine dimer. The highest barrier was found to be for the regeneration of the adenosyl radical.

Acknowledgements

I thank the following persons for valuable discussions: Prof. Per Siegbahn, Prof. Yi Luo, Prof. Jeremy Harvey, Jing-Dong Guo, and Arianna Bassan. The Wenner-Gren Foundations is acknowledged for financial support.

References

[1] A.D. Becke, Density-functional exchange-energy approximation with correct asymptotic behavior, Phys. Rev. A38 (1988) 3098.
[2] A.D. Becke, Density-functional thermochemistry: 1. The effect of the exchange-only gradient correction, J. Chem. Phys. 96 (1992) 2155.
[3] A.D. Becke, Density-functional thermochemistry: 2. The effect of the Perdew–Wang generalized-gradient correlation correction, J. Chem. Phys. 97 (1992) 9173.
[4] A.D. Becke, Density-functional thermochemistry: 3. The role of exact exchange, J. Chem. Phys. 98 (1993) 5648.
[5] C.W. Bauschlicher Jr., A. Ricca, H. Partridge, S.R. Langhoff, Chemistry by density functional theory, in: D.P. Chong (Ed.), Recent Advances in Density Functional Methods, Part II, World Scientific Publishing, Singapore, 1997, p. 165.
[6] F. Himo, P.E.M. Siegbahn, Quantum chemical studies of radical-containing enzymes, Chem. Rev. 103 (2003) 2421.
[7] P.E.M. Siegbahn, M.R.A. Blomberg, Density functional theory of biologically relevant metal centers, Annu. Rev. Phys. Chem. 50 (1999) 221.
[8] P.E.M. Siegbahn, M.R.A. Blomberg, A quantum chemical approach to the study of reaction mechanisms of redox-active metalloenzymes, J. Phys. Chem., B 105 (2001) 9375.
[9] P.E.M. Siegbahn, Mechanisms of metalloenzymes studied by quantum chemical methods, Q. Rev. Biophys. 36 (2003) 91.
[10] T. Lovell, F. Himo, W.-G. Han, L. Noodleman, Density functional methods applied to metalloenzymes, Coord. Chem. Rev. 238–239 (2003) 211.
[11] J. Knappe, F.A. Neugebauer, H.P. Blaschkowski, M. Gänzler, Post-translational activation introduces a free-radical into pyruvate formate-lyase, Proc. Natl. Acad. Sci. U. S. A. 81 (1984) 1332.
[12] A.F.V. Wagner, M. Frey, F.A. Neugebauer, W. Schafer, J. Knappe, The free radical in pyruvate formate-lyase is located on glycine-734, Proc. Natl. Acad. Sci. U. S. A. 89 (1992) 996.
[13] V.-M. Leppänen, M.C. Merckel, D.L. Ollis, K.K. Wong, J.W. Kozarich, A. Goldman, Pyruvate formate lyase is structurally homologous to type I ribonucleotide reductase, Structure 7 (1999) 733.
[14] A. Becker, K. Fritz-Wolf, W. Kabsch, J. Knappe, S. Schultz, A.F.V. Wagner, Structure and mechanism of the glycyl radical enzyme pyruvate formate-lyase, Nat. Struct. Biol. 6 (1999) 969.
[15] A. Becker, W. Kabsch, X-ray structure of pyruvate formate-lyase in complex with pyruvate and CoA, J. Biol. Chem. 277 (2002) 40036.
[16] F. Himo, L.A. Eriksson, Catalytic mechanism of pyruvate formate-lyase; a theoretical study, J. Am. Chem. Soc. 120 (1998) 11449.
[17] F. Himo, Stability of protein-bound glycyl radical, a density functional theory study, Chem. Phys. Lett. 328 (2000) 270.
[18] F. Himo, L.A. Eriksson, On the local geometry of glycyl radicals in different enzymes, J. Chem. Soc., Perkin Trans. 2 (2) (1998) 305.
[19] E.J. Brush, K.A. Lipsett, J.W. Kozarich, Inactivation of *Escherichia coli* pyruvate formate-lyase by hypophosphite: evidence for a rate-limiting phosphorus-hydrogen bond cleavage, Biochemistry 27 (1988) 2217.
[20] C.V. Parast, K.K. Wong, S.A. Lewisch, J.W. Kozarich, J. Peisach, R.S. Magliozzo, Hydrogen exchange of the glycyl radical of pyruvate formate-lyase is catalyzed by cysteine 419, Biochemistry 34 (1995) 2393.
[21] J.-D. Guo, F. Himo, in preparation.
[22] R.A. Mehl, T.P. Begley, Mechanistic studies on the repair of a novel DNA photolesion: the spore photoproduct, Org. Lett. 1 (1999) 1065.
[23] R. Rebeil, W.L. Nicholson, The subunit structure and catalytic mechanism of the *Bacillus subtilis* DNA repair enzyme spore photoproduct lyase, Proc. Natl. Acad. Sci. U. S. A. 98 (2001) 9038.
[24] J. Cheek, J.B. Broderick, Direct H atom abstraction from spore photoproduct C-6 initiates DNA repair in the reaction catalyzed by spore photoproduct lyase: evidence for a reversibly generated adenosyl radical intermediate, J. Am. Chem. Soc. 124 (2002) 2860.
[25] J.-D. Guo, Y. Luo, F. Himo, DNA repair by spore photoproduct lyase; a density functional theory study, J. Phys. Chem., B. 107 (2003) 11188.
[26] B. Leuthner, C. Leutwein, H. Schulz, P. Hörth, W. Haehnel, E. Schilz, H. Schägger, J. Heider, Biochemical and genetic characterization of benzylsuccinate synthase from thauera aromatica: a new glycyl radical enzyme catalysing the first step in anaerobic toluene metabolism, Mol. Microbiol. 28 (1998) 615.
[27] C.J. Krieger, W. Roseboom, S.P.J. Albracht, A.M. Spormann, A stable organic free radical in anaerobic benzylsuccinate synthase of *Azoarcus* sp. strain T, J. Biol. Chem. 276 (2001) 12924.
[28] F. Himo, Catalytic mechanism of benzylsuccinate synthase. A theoretical study, J. Phys. Chem., B. 106 (2002) 7688.